

## Recovery Behavior of Si(Li) Junctions after Gamma Irradiation\*

C. A. J. AMMERLAAN

*Natuurkundig Laboratorium, Universiteit van Amsterdam, Amsterdam, The Netherlands*

(Received 24 May 1968; in final form 23 August 1968)

An investigation was made into the room-temperature recovery behavior of lithium-drifted  $p^+-i-n^+$  junctions in silicon after irradiation with  $^{60}\text{Co}$  gamma rays. In most cases, the effects due to irradiation were detected by measuring the capacity vs reverse voltage characteristics of the junctions. Negative space charge appears to be created by precipitation of lithium donors on irradiation defects. The relaxation time associated with this interaction is determined by a capture radius of  $(4\pm 1)\times 10^{-8}$  cm. In reverse-biased junctions, space charge is neutralized by lithium-ion drift. This compensation process, also observed in lithium-diffused  $p-n$  junctions, is characterized by the ionic relaxation time. Expressions, relating both time constants to properties of the basic silicon, are given.

### INTRODUCTION

The research reported on in this paper and in two previous ones,<sup>1,2</sup> was carried out to advance the understanding of irradiation effects in lithium-drifted  $p^+-i-n^+$  junctions. In these junctions, with planar geometry, the three adjoining respective regions are: (a) a low-resistivity  $p^+$ -type, boron-doped, layer, (b) a carefully compensated layer, intrinsic at room temperature, 1 or 2 mm wide, (c) a low-resistivity  $n^+$ -type, heavily lithium-doped layer.

The intrinsic region is produced by close balancing of boron acceptors by lithium donors using lithium ion drift in a reverse-biased junction. After the principle of this method had been investigated by Pell,<sup>3</sup> various authors have treated the actual preparation of lithium-drifted junctions.<sup>4-6</sup>  $p^+-i-n^+$  junctions are widely applied as nuclear radiation detectors, for which they have excellent qualifications.<sup>7</sup> Being functionally exposed to radiation, the matter of irradiation damage in these junctions is raised automatically. In particular the high degree of compensation, characterizing the intrinsic region, is easily upset by irradiation produced electrically active defects.

It therefore seemed worthwhile, both from an applied and a more fundamental point of view, to study the irradiation effects in lithium-drifted  $p^+-i-n^+$  junctions. A relatively simple form of damage was produced by irradiation with the 1.17 and 1.33 MeV gammas from a  $^{60}\text{Co}$  source.<sup>8</sup> Irradiations were performed with the samples at liquid-nitrogen temperature or near  $0^\circ\text{C}$ .

Through intermediate Compton electrons the photons create interstitial silicon atoms and vacancies.

These so-called primary defects are unstable at room temperature. They diffuse through the silicon lattice until stable defects are formed by association with chemical impurities or other lattice imperfections. Uniform damage is introduced because the penetration depth of the gammas is large compared to actual sample dimensions. The irradiation effect is detected by the production of uniform space charge in the compensated region, the intrinsic silicon being transformed into extrinsic. The present paper deals with observations made in twelve samples of the time dependence of this space charge near room temperature.

Samples were irradiated to an integrated dose of  $3\times 10^{15}$   $\gamma/\text{cm}^2$ . Cross sections for defect production for room-temperature irradiations were near  $5\times 10^{-4}$  defect/ $\gamma\cdot\text{cm}$ , which was about three times larger than the values observed after irradiations performed at liquid-nitrogen temperature. Near  $10^{12}$  defects/ $\text{cm}^3$  were consequently introduced in our samples. This defect yield turned out to be hardly dependent upon the nature of the main impurity present in the silicon crystals.

The initial material, from which  $p^+-i-n^+$  junctions were prepared, was  $p$ -type, boron-doped, single-crystal silicon. It was obtained from various suppliers, including Merck, Sharp and Dohme (M), Wacker Chemie (W), and Texas Instruments Inc. (TI).<sup>9</sup> Some measurements, carried out to determine the properties of this basic material, are described in the next section.

### INVESTIGATION OF THE BASIC SILICON

#### 1. Dislocation Density

By determining the etch-pit density the number of dislocations per unit area could be easily estimated. Counts of etch pits, produced by the methods of Dash<sup>10</sup> or Sirtl,<sup>11</sup> led to the results as shown in Table I. It seems that the dislocation density has no significance for the

\* This work formed part of the research program of the Foundation for Fundamental Research of Matter (F.O.M.), made possible by financial support from the Netherlands Organization for the Advancement of Pure Research (Z.W.O.).

<sup>1</sup> C. A. J. Ammerlaan, *Effets des Rayonnements sur les Semiconducteurs* (Dunod Cie, Paris, France, 1965), p. 295.

<sup>2</sup> C. A. J. Ammerlaan, thesis, University of Amsterdam (1967).

<sup>3</sup> E. M. Pell, *J. Appl. Phys.* **31**, 291 (1960).

<sup>4</sup> J. H. Elliott, *Nucl. Instr. Methods* **12**, 60 (1961).

<sup>5</sup> J. W. Mayer, *J. Appl. Phys.* **33**, 2894 (1962).

<sup>6</sup> C. A. J. Ammerlaan and K. Mulder, *Nucl. Instr. Methods* **21**, 97 (1963).

<sup>7</sup> G. Dearnaley and D. C. Northrop, *Semiconductor Counters for Nuclear Radiations* (Spon Limited, London, England, 1964).

<sup>8</sup> Hospitality received from the "Antoni van Leeuwenhoekhuis," where all irradiations were performed, was highly appreciated.

<sup>9</sup> Silicon from Texas Instruments Inc. was sold under the trademark "Lopex."

<sup>10</sup> W. C. Dash, *J. Appl. Phys.* **30**, 459 (1959).

<sup>11</sup> E. Sirtl and A. Adler, *Z. Metallk.* **52**, 529 (1961).

TABLE I. Typical data for the basic silicon. Etch-pit density EPD, boron concentration  $n_B$ , compensating donor concentration  $n_d$ , oxygen concentration  $n_o$ , and fraction of free lithium ions  $\alpha$  for some temperatures  $T$  for one sample taken from each of the four batches.

| Sample    | EPD<br>(cm <sup>-2</sup> ) | $n_B$<br>(10 <sup>14</sup><br>cm <sup>-3</sup> ) | $n_d$<br>(10 <sup>14</sup><br>cm <sup>-3</sup> ) | $n_o$<br>(10 <sup>14</sup><br>cm <sup>-3</sup> ) | $T$<br>(°C) | $\alpha$ |
|-----------|----------------------------|--|--|--|-------------|----------|
| M, 7, 12  | 30 000                     | 1.55   | 0.16   | <10  | -10         | 0.80     |
|           |                            |  |  |  | 0           | 0.78     |
|           |                            |  |  |  | +10         | 0.76     |
|           |                            |  |  |  | +20         | 0.76     |
|           |                            |  |  |  | +30         | 0.84     |
| TI, 1, 11 | 500                        | 3.29   | 1.66   | 75   | +20         | 0.28     |
|           |                            |  |  |  | +40         | 0.48     |
| TI, 2, 6  | 1 300                      | 7.71   | 0.67   | 620  | +10         | 0.017    |
|           |                            |  |  |  | +20         | 0.032    |
|           |                            |  |  |  | +30         | 0.047    |
|           |                            |  |  |  | +40         | 0.081    |
|           |                            |  |  |  | +50         | 0.123    |
|           |                            |  |  |  | +60         | 0.171    |
| W, 2, 5   | 24 000                     | 15.2   | 0.02   | <10  | +30         | 0.28     |

interpretation of the irradiation induced effects. These examinations are, however, useful for the elimination of crystals exhibiting gross structural defects.

## 2. Resistivity and Hall Effect

Concentrations of electrically active dopants of the silicon were determined by measurements of resistivity and Hall effect. These experiments were carried out according to the method developed by Van der Pauw,<sup>12</sup> in a temperature range from about 20°–300°K. Results of the measurements, carrier concentration versus temperature, were analyzed on a model allowing for compensating donors. The analysis yields an identification of the acceptor as boron ions, their concentration  $n_B$  and the total donor concentration  $n_d$ . In the intrinsic region of the  $p^+-i-n^+$  junctions, to be prepared in this silicon, the lithium concentration  $n_{Li}$  will be equal to the net acceptor concentration  $n_B - n_d$ . As will become clear in following sections, the resistivity and Hall-effect measurements are directly related to the interpretation of the time dependence of the irradiation-induced phenomena.

## 3. Oxygen Concentration

It is known that lithium interacts with both boron<sup>13</sup> and oxygen<sup>14</sup> in forming a complex defect structure. Therefore, also the concentration of the latter impurity is of importance. A specific investigation to the presence of oxygen is enabled by an associated vibrational ir

<sup>12</sup> L. J. van der Pauw, Philips Res. Rept. **13**, 1 (1958).  
<sup>13</sup> H. Reiss, C. S. Fuller, and F. J. Morin, Bell System Tech. J. **35**, 535 (1956).  
<sup>14</sup> E. M. Pell, *International Conference on Solid State Physics in Electronics and Telecommunications, Brussels, 1958* (Academic Press Inc., New York, 1960), Vol. I, p. 261.

absorption, which occurs at a wavelength of approximately 9  $\mu\text{m}$ .<sup>15,16</sup> Measurements were performed at liquid-helium temperature, since the sensitivity of the method is highest, and the limit of detectability, estimated at 10<sup>15</sup> oxygen atoms per cm<sup>3</sup>, is lowest at this temperature.

## 4. Lithium Drift in $p-n$ Junction

In an intermediate stage of the preparation of a  $p^+-i-n^+$  junction lithium is introduced into the  $p$ -type silicon by diffusion. A relatively thin layer of the silicon slice is then  $n$ -type counterdoped and a  $p-n$  junction is formed. Valuable information is obtained by measuring the lithium ion-drift rate in this reverse-biased  $p-n$  junction. Based on a linear spatial distribution of lithium impurities Pell<sup>3</sup> derived the formula:

$$(d \ln C / dt)_{t=0} = -1/3\tau_C, \quad (1)$$

expressing, for time  $t=0$ , the rate of change of the capacity  $C$  of the junction. The time constant  $\tau_C$ , which we call ionic relaxation time, is given by:

$$\tau_C = \epsilon / n_{Li} e \mu_{Li}, \quad (2)$$

where  $\epsilon = \epsilon_0 \epsilon_r$  is the dielectric constant ( $\epsilon_r = 11.8$ ) and  $e$  the electronic charge. The lithium concentration in the drift region equals the net acceptor concentration determined by the resistivity and Hall-effect measurements. Since also the mobility of lithium ions in silicon  $\mu_{Li}$  is known,<sup>17,18</sup> the ionic relaxation time  $\tau_C$  may be calculated straightforward and compared to the experimental findings.

Under usual diffusion conditions the lithium distribution is given by a complementary error function and deviates slightly from the assumed linear dependence. A correction factor validating the formula for this actual lithium distribution is required.<sup>2</sup> If interactions with boron,  $\text{Li}^+ + \text{B}^- \rightleftharpoons \text{LiB}$ , or with oxygen,  $\text{Li}^+ + \text{O} \rightleftharpoons \text{LiO}^+$ , are present part of the lithium ions is bound into immobile complexes. This, of course, results in a reduced effective drift rate and an apparent increase of ionic relaxation time. One can take this effect into account by introducing the factor  $\alpha$ , equal to the fraction of free, unpaired lithium ions. As are the equilibrium constants of the reactions,<sup>19–22</sup> the fraction  $\alpha$  is a function of temperature. If all concentrations of the impurities involved are known then  $\alpha$  may be calculated.

<sup>15</sup> W. Kaiser, P. H. Keck, and C. F. Lange, Phys. Rev. **101**, 1264 (1956).

<sup>16</sup> H. J. Hrostowski and B. J. Alder, J. Chem. Phys. **33**, 980 (1960).

<sup>17</sup> E. M. Pell, Phys. Rev. **119**, 1222 (1960).

<sup>18</sup> E. M. Pell, Phys. Rev. **119**, 1014 (1960).

<sup>19</sup> E. M. Pell, J. Appl. Phys. **31**, 1675 (1960).

<sup>20</sup> F. A. Kröger, *The Chemistry of Imperfect Crystals* (North-Holland Publishing Company, Amsterdam, The Netherlands, 1964), p. 271.

<sup>21</sup> W. G. Spitzer and M. Waldner, Phys. Rev. Letters **14**, 223 (1965).

<sup>22</sup> E. M. Pell, J. Appl. Phys. **32**, 1048 (1961).

A summary of results is given in Table I. For the sake of brevity only data for one slice per batch are tabulated. These may be considered as typical values for all slices of the same batches. The M,7-samples are sufficiently pure for  $\alpha$  to be near unity. On the other hand, the oxygen contamination in the TI-samples reduces  $\alpha$  considerably. In the W,2-samples the reduction of  $\alpha$  is due to lithium-boron ion pairing.

## DETECTION OF THE IRRADIATION EFFECT

### 1. Potential Probe

Using a potential probe the electrostatic potential distribution  $\phi(x)$  in a reverse-biased junction could be measured along a lateral face of the slices, traversing

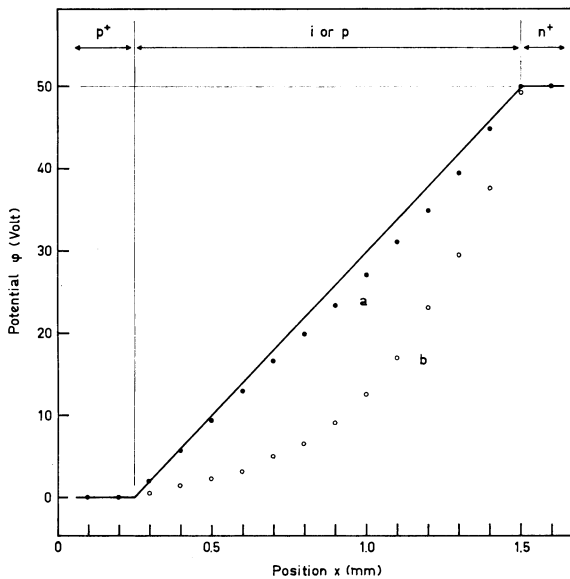


FIG. 1. Potential  $\phi$  against position  $x$  in a junction with reverse bias of 50 V; (a)  $p^+-i-n^+$  junction before irradiation ( $\bullet$ ), (b)  $p^+-p-n^+$  junction after irradiation ( $\circ$ ). Heavily drawn straight lines are theoretical for  $p^+-i-n^+$  junction.

from  $p^+$ - to  $n^+$ -type regions. With reference to Poisson's equation,  $d^2\phi/dx^2 = -\rho/\epsilon$ , obviously the space-charge  $\rho$  may be determined by this method. Results are shown in Fig. 1. Before irradiation no net space charge exists in the  $i$  region of the junction and accordingly the potential increases nearly linearly with position. After irradiation the concave shape of the measured  $\phi(x)$  curve indicates an irradiation produced negative space charge. Attempts to determine the amount of space charge quantitatively by the potential probe method were not successful because surface inversion problems could not be overcome sufficiently.

### 2. Particle Detection

To investigate the effects of irradiation by detection of nuclear particles, a junction was drifted so far that

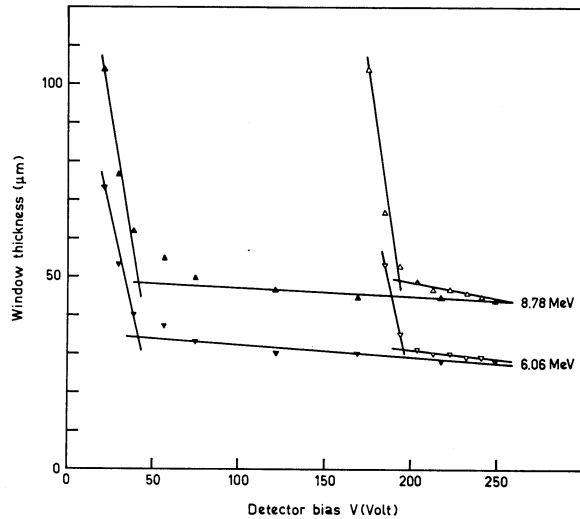


FIG. 2. Window thickness observed by detection of  $\alpha$ -particles from the radioactive source  $^{212}\text{Pb}$  in a  $p^+-i-n^+$  junction before irradiation (filled-in triangles) or in a  $p^+-p-n^+$  junction after irradiation (open triangles).

almost all  $p^+$ -type silicon was compensated. Particles were directed perpendicular upon the remaining  $p^+$ -type layer, which was relatively thin compared to incident particle ranges. Pulse heights were then recorded as function of detector reverse bias. In this way, it is possible to locate the  $p$ - to  $n$ -type transition and to deduce whether the  $p^+-i-n^+$  junction character has been changed into  $p^+-p-n^+$  or  $p^+-n-n^+$  by the irradiation. Also, the voltage  $V_m$ , required to deplete the irradiated junction to its original intrinsic width, may be determined.

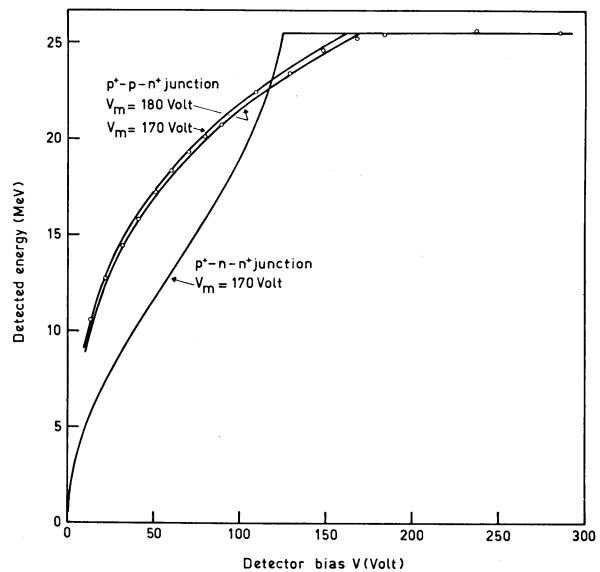


FIG. 3. Detection of 26 MeV deuterons by an irradiated junction. Experimental points:  $\circ$ . Drawn lines are calculated assuming a value for  $V_m$ .

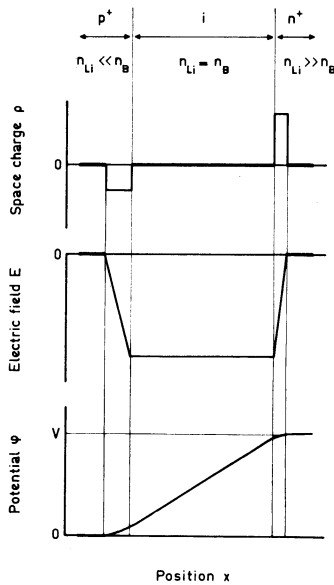


FIG. 4. Schematic of space charge  $\rho$ , electric field  $E$ , and potential  $\phi$  versus position  $x$  in a  $p^+-i-n^+$  junction with reverse bias  $V$ ;  $n_{Li}$ =lithium concentration,  $n_B$ =boron concentration.

These experiments were carried out using the 6.06 and 8.78 MeV  $\alpha$ -particles of the natural source  $^{212}\text{Pb}$ . Effective window thicknesses, calculated from observed pulse-height attenuations, are given as function of reverse bias in Fig. 2. Results indicate  $p^+-p-n^+$  character of the irradiated junction and a depletion voltage  $V_m$  near 190 V. More detailed information was obtained by employing 26 MeV cyclotron accelerated

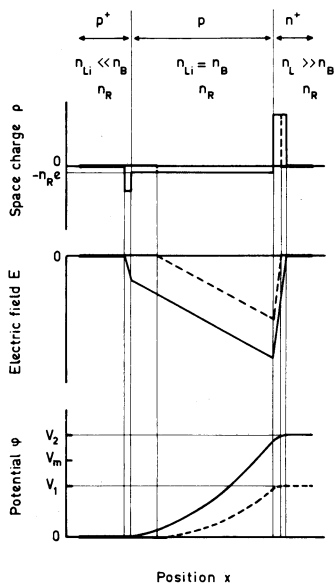


FIG. 5. Schematic of space charge  $\rho$ , electric field  $E$ , and potential  $\phi$  versus position  $x$  in a  $p^+-p-n^+$  junction with reverse bias  $V_1 < V_m$  (dashed lines) and  $V_2 > V_m$  (drawn lines);  $n_R$ =irradiation defect density.

deuterons.<sup>23</sup> Since the range of these particles is comparable with the junction width a larger part of the junction volume is probed. Results, as shown in Fig. 3, are only consistent with a  $p^+-p-n^+$  junction character and fix the depletion voltage  $V_m$  at about 175 V.

### 3. Capacity Measurements

Detection of the irradiation-produced space charge was mainly made by measuring the capacity dependence upon reverse bias. A small 10 kHz oscillating voltage was applied in series with the dc reverse bias. By careful shielding, parallel capacity of connecting leads was eliminated. Some electrical parameters, space charge  $\rho$ , electric field  $E$ , and potential  $\phi$  are plotted

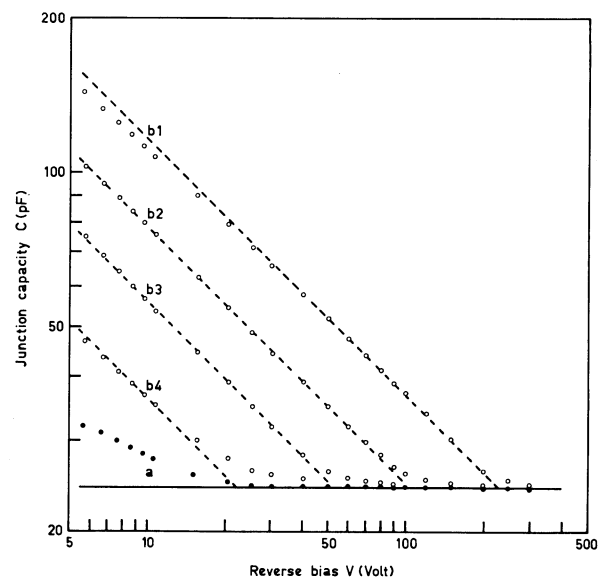


FIG. 6. The capacity  $C$  as function of reverse bias  $V$  for: (a)  $p^+-i-n^+$  junction before irradiation ( $\bullet$ ), (b1)-(b4)  $p^+-p-n^+$  junction after irradiation ( $\circ$ ). Horizontal drawn line is calculated from drift data; dashed lines are drawn with slope  $-1/2$  for comparison of experimental results with theory.

against position  $x$  for a  $p^+-i-n^+$  junction in Fig. 4. The depleted junction width  $W_m$  is almost equal to the thickness of the intrinsic region, independent of reverse bias. The junction capacity  $C_m$ , given by  $C_m = \epsilon A / W_m$ , is therefore in practice a constant, as shown by curve (a) of Fig. 6. Electrical conditions in the irradiated junction, the  $p^+-p-n^+$  junction, are illustrated in Fig. 5. The capacity vs reverse voltage curve now consists of two straight lines. For low reverse bias,  $V < V_m$ , the junction is not depleted to the maximum width  $W_m$ . Because of the uniform space charge in the  $p$  region, the depleted layer thickness increases according to the square root of the applied bias and consequently, the capacity  $C$  is proportional to  $V^{-1/2}$ . This behavior is demonstrated by

<sup>23</sup> Permission to perform this experiment at the "Instituut voor Kernfysisch Onderzoek" is gratefully acknowledged.

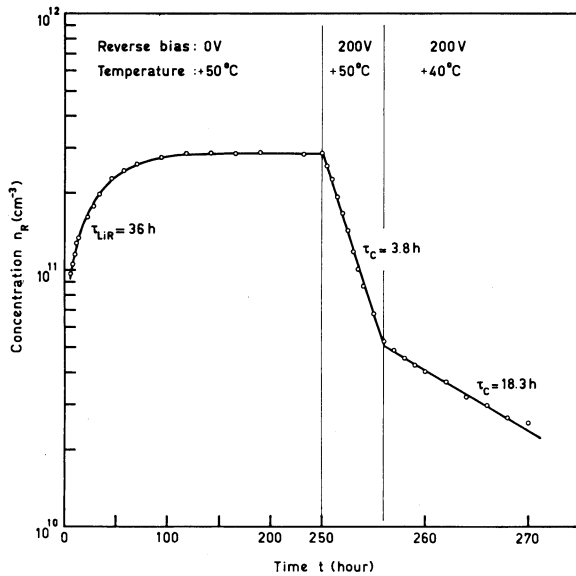


FIG. 7. Variation of defect concentration in sample TI, 2, 1 as function of time under various conditions of temperature and reverse bias. Note change of time scale at  $t=250$  h. Drawn lines are calculated using the formulas (3) or (6), and the stated values for the time constants.

the curves (b1-b4) of Fig. 6. Assuming singly ionized defects, their concentration  $n_R$  is calculated from

$$n_R = 2C_m^2 V_m / e\epsilon A^2.$$

Concluding this discussion on the detection methods a comparison may be made between the various results. Table II lists the values of  $V_m$  obtained on one junction by capacity measurements and particle detection.

## TIME DEPENDENCE

### 1. Space-Charge Generation

Always an increase of space charge was observed if irradiated junctions were left without reverse bias near room temperature. This process could be described reasonably well by the expression

$$\rho(t) = \rho(\infty) [1 - \exp(-t/\tau_{LiR})], \quad (3)$$

which forms a solution to the differential equation:

$$d\rho/dt = [\rho(\infty)/\tau_{LiR}] \cdot \exp(-t/\tau_{LiR}). \quad (4)$$

TABLE II. Determination of the depletion voltage  $V_m$  by various methods.

| Method of measurement                          | $V_m$ (V) |
|--|-----------|
| $^{212}\text{Pb}$ $\alpha$ -particles 6.06 MeV | 180       |
| $^{212}\text{Pb}$ $\alpha$ -particles 8.78 MeV | 181       |
| Cyclotron deuterons 26 MeV                     | 175       |
| Junction capacity                              | 172       |

TABLE III. Summary of data on the time constant  $\tau_{LiR}$ .

| Sample    | Temperature (°C) | $\alpha$ | $\tau_{LiR}$ (h) | $R_{\text{capd}}$ ( $10^{-8}$ cm) |
|-----------|------------------|----------|------------------|-----------------------------------|
| M, 7, 6   | 19               | 0.8      | 450              | 3.4                               |
| M, 7, 11  | 30               | 0.84     | 183              | 3.1                               |
| M, 7, 13  | 30               | 0.8      | 150              | 4.0                               |
|           | 40               | 0.8      | 65               | 4.2                               |
|           | 50               | 0.8      | 22               | 5.9                               |
| M, 7, 14  | 30               | 0.8      | 143              | 4.2                               |
|           | 50               | 0.8      | 31               | 4.1                               |
| TI, 1, 11 | 40               | 0.48     | 120              | 3.3                               |
| TI, 2, 1  | 20               | 0.026    | 1850             | 4.9                               |
|           | 30               | 0.044    | 500              | 4.5                               |
|           | 40               | 0.071    | 160              | 3.9                               |
|           | 50               | 0.109    | 36               | 5.4                               |
| TI, 2, 6  | 30               | 0.047    | 700              | 3.0                               |
|           | 50               | 0.123    | 42               | 4.1                               |

Saturation of space-charge creation is shown in the left part of Fig. 7, where  $n_R(t) = \rho(t)/e$  is plotted. The phenomena are explained by assuming precipitation of lithium ions on irradiation defects in the reaction:  $\text{Li}^+ + \text{R} \rightarrow \text{LiR}$ . If the complex LiR is a neutral defect, the loss of lithium donors results in net acceptors,  $p$ -type behavior therefore, and negative space charge. First-order kinetics, as actually observed, are expected for this process since  $n_R \ll n_{Li}$ . For the above-mentioned diffusion limited reaction the time constant

TABLE IV. Summary of data on the time constant  $\tau_C$ . Numbers stated in the fourth column were calculated from the results of lithium-ion drift in the  $p$ - $n$  junction. The values for  $\tau_C$  given in the last column were actually observed in the compensation of  $p^+ - p - n^+$  junctions.

| Sample    | Temperature (°C) | $\alpha$ | $\tau_C$ calc (h) | $\tau_C$ meas (h) |
|-----------|------------------|----------|-------------------|-------------------|
| M, 7, 6   | 19               | 0.8      | 32                | 30                |
| M, 7, 11  | 30               | 0.84     | 12.2              | 11.7              |
| M, 7, 12  | 30               | 0.84     | 12.2              | 12.4              |
| M, 7, 13  | 40               | 0.8      | 6.1               | 6.7               |
| M, 7, 14  | 60               | 0.9      | 1.31              | 1.35              |
| TI, 1, 4  | 30               | 0.38     | 24.5              | 22.0              |
| TI, 1, 11 | 40               | 0.48     | 8.6               | 8.5               |
| TI, 2, 1  | 40               | 0.07     | 14.2              | 18.3              |
|           | 50               | 0.11     | 5.2               | 3.8               |
| TI, 2, 6  | 30               | 0.047    | 45.6              | 48                |
|           | 40               | 0.081    | 12.2              | 11.5              |
|           | 50               | 0.123    | 3.9               | 3.6               |
| W, 2, 3   | 20               | 0.17     | 11.1              | 11.2              |
| W, 2, 5   | 20               | 0.25     | 8.8               | 7.9               |

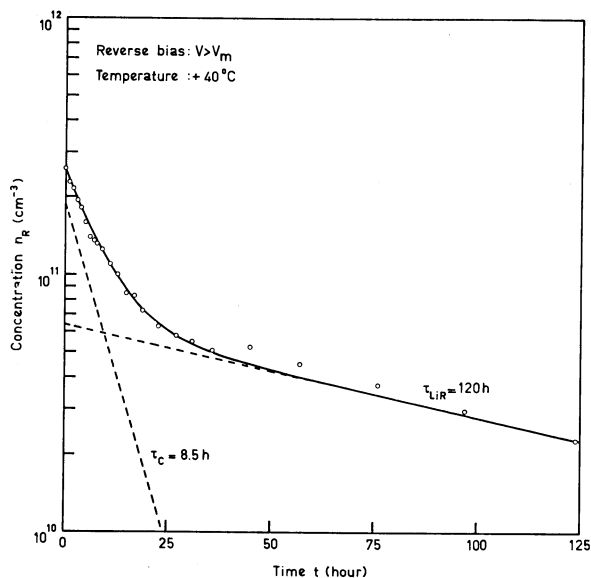


FIG. 8. Variation of defect concentration in sample TI, 1, 11 as function of time in the reverse-biased junction. Drawn line is calculated by using formula (8).

$\tau_{LiR}$  is given by<sup>13,24</sup>

$$\tau_{LiR} = (4\pi\alpha n_{Li} D_{Li} R_{capt})^{-1}.$$

The only unknown parameter in this formula, the capture radius  $R_{capt}$ , may be calculated from the experimental data. From Table III, which summarizes the results, it follows that under a variety of experimental conditions the capture radius assumes the rather constant value of  $R_{capt} = (4 \pm 1) \times 10^{-8}$  cm. Since this is a reasonable value for a process lacking long range Coulomb attraction the adopted model is confirmed.

## 2. Space-Charge Compensation

Application of a reverse bias  $V > V_m$  across the junctions starts a process of space charge compensation by lithium ion drift. A mathematical formulation of this process follows from the Poisson, transport, and continuity equations and appropriate boundary conditions.<sup>2</sup> The result reads

$$d \ln \rho / dt = -1/\tau_C, \quad (5)$$

where the ionic relaxation time is again given by (2). This result is very similar to Eq. (1) governing the lithium ion-drift compensation in  $p-n$  junctions, the difference by a factor three being related to the assumed linear space charge distribution in the  $p-n$  junction case.

<sup>24</sup> T. R. Waite, J. Chem. Phys. **32**, 21 (1960).

Equation (5) has for its solution

$$\rho(t) = \rho(0) \exp(-t/\tau_C). \quad (6)$$

The exponential decrease of space charge is also shown in Fig. 7, for two different temperatures. Numerical values are stated in Table IV, where values for  $\tau_C$  obtained by lithium-ion drift in the  $p-n$  and  $p^+-p-n^+$  junctions are compared.

The time constant  $\tau_C$  is called ionic relaxation time by analogy with the dielectric relaxation time, since it is the  $RC$ -time of a junction for the electric transport properties of the lithium ions. The ionic relaxation time is the product of the capacity  $\epsilon$  of a junction of unit dimensions and its resistance  $1/n_{Li}e\mu_{Li}$ . Besides, it may be easily shown, that  $\tau_C$  is identical with  $\tau_{LiR}$  in the special case that the capture radius  $R_{capt}$  equals the Coulomb capture radius  $R_C = e^2/4\pi\epsilon kT$ .

## 3. Combined Generation and Compensation

In case space-charge generation and compensation are simultaneously present in a reverse-biased junction, the mathematical description is simply obtained by combining the Eqs. (4) and (5), yielding

$$d\rho/dt = -\rho(t)/\tau_C + [\rho(\infty)/\tau_{LiR}] \cdot \exp(-t/\tau_{LiR}). \quad (7)$$

The solution is:

$$\rho(t) = [\rho(0) - \rho(\infty) \cdot \tau_C / (\tau_{LiR} - \tau_C)] \exp(-t/\tau_C) + \rho(\infty) \cdot \tau_C / (\tau_{LiR} - \tau_C) \cdot \exp(-t/\tau_{LiR}). \quad (8)$$

Behavior of this type is demonstrated in Fig. 8, where the analysis, according to the above formula, is made as a sum of two exponential functions.

## SUMMARY

It is shown that by gamma irradiation a lithium-drifted  $p^+-i-n^+$  junction is converted into a  $p^+-p-n^+$  junction. This is caused by loss of lithium donors, which precipitate on irradiation defects creating electrically inactive centers. The self-healing properties by lithium-ion drift in the reverse-biased junctions are demonstrated. Space-charge neutralization in  $p-n$  junctions and  $p^+-p-n^+$  junctions are closely related. The time dependence of space-charge generation and compensation is quantitatively described.

## ACKNOWLEDGMENTS

Drs. J. P. Woerdman, Drs. J. J. Goedbloed, Drs. P. H. Schipper, and W. H. Kool contributed materially to this work. Discussions with Professor Dr. G. de Vries, especially in the adaptation of the data as a thesis, were very much appreciated.